World Electric Vehicle Journal

Article

Comparison and Analysis of Electromagnetic Characteristics of Basic Structure of Wireless Power Coil for Permanent Magnet Motors in Electric Vehicles

Junfeng Zhao [1,2,*], Lingyun Zhao [3], Yuwei Zou [4] and Tianjin Chen [5]

[1] Key Laboratory of Mold Intelligent Manufacturing of Taizhou, Taizhou 318020, China
[2] School of Mechatronics and Mould Engineering, Taizhou Vocational College of Science & Technology, Taizhou 318020, China
[3] School of Mechanical Engineering, Dalian University of Technology, Dalian 116023, China
[4] School of Physics and Electrical Engineering, Anyang Normal University, Anyang 455000, China
[5] Xuji Power Co., Ltd., Xuchang 461000, China
* Correspondence: zhao.zjf@gmail.com

Abstract: The purpose of this paper is to compare and analyze the electromagnetic characteristics of the basic structure of the coil in the electromagnetic coupling mechanism for the wireless power supply of permanent magnet motors in electric vehicles. The electromagnetic coupling mechanism is one of the key technologies for wireless power transmission and the coil structure plays a key role in the transmission performance of the coupling mechanism, and different structures can achieve different performances. The central objective of coil structure studies is to investigate how the coupling coefficient can be increased to achieve greater transmitted power and higher efficiency. In this paper, we investigate two basic coil configurations, circular and square, by studying their flux density variations when used as transmitting coils and their electromagnetic coupling characteristics when used as receiving coils. Three couplers consisting of circular and square coils are also analyzed in simulations and experiments are carried out on couplings containing circular and square coils of the same area. The results of the study show that the qualitative analysis, simulation analysis and experimental results are in high agreement. The results of this paper are an important reference for the design and optimization of wireless power coils for permanent magnet motors in electric vehicles.

Keywords: basic coil structure; electromagnetic characteristics; qualitative analysis; wireless power transfer

check for updates

Citation: Zhao, J.; Zhao, L.; Zou, Y.; Chen, T. Comparison and Analysis of Electromagnetic Characteristics of Basic Structure of Wireless Power Coil for Permanent Magnet Motors in Electric Vehicles. *World Electr. Veh. J.* **2023**, *14*, 199. https://doi.org/10.3390/wevj14080199

Academic Editor: Ziqiang Zhu

Received: 6 June 2023
Revised: 17 July 2023
Accepted: 21 July 2023
Published: 26 July 2023

1. Introduction

With the popularization of electric vehicles and advancements in wireless power transfer technology, magnetic field-coupled static wireless charging technology has attracted significant attention in the field of electric vehicles. However, charging issues still remain one of the main bottlenecks in the development of electric vehicles. Therefore, researchers are actively exploring the possibility of wireless power transfer for electric vehicle permanent magnet motors [1–4].

As a hot topic in current research, there are still many unresolved issues regarding the coupling mechanism of wireless charging technology for electric vehicles. Some of these issues include the design of high-power coupling mechanisms suitable for fast charging modes, improving efficiency, reducing size and achieving lightweight construction.

The electromagnetic coupling mechanism is one of the key technologies for wireless power supply, and coil parameters are critical factors that affect the performance of the coupling mechanism. The coil structure plays a crucial role in the transmission performance, and different structures can achieve different performance characteristics [5–7]. The power transfer efficiency is not directly proportional to the coil size, and it needs to be analyzed on a case-by-case basis. Optimal coil parameters should be determined to achieve efficient power transmission while ensuring high-power transfer capability. In designing coils, studying how to improve the coupling coefficient is a crucial objective. A higher coupling coefficient implies higher transmission power and greater efficiency.

Researchers have already investigated circular pad couplers and found that the basic magnetic flux path within the pad remains relatively fixed [8]. Therefore, to enhance the coupling efficiency of coils, further research is needed into other coil structures and design methods. In 2010, the University of Auckland proposed a coil design called “Flux Pipe” based on their research on the magnetic field characteristics of circular coil pads, as shown in Figure 1. This design utilizes a dual-coil structure where two coils are connected in parallel, and the magnetic flux generated by the two coils is connected in series within the magnetic circuit. As a result, the design enhances the horizontal displacement tolerance [9]. In 2012, Saitama University in Japan introduced a transformer design called the “H-coil”. This coil design is compact and tightly arranged, resulting in a smaller size, as shown in Figure 2. Additionally, the magnetic field of the coil is located on both sides of the coil, providing strong resistance against displacement [9,10].

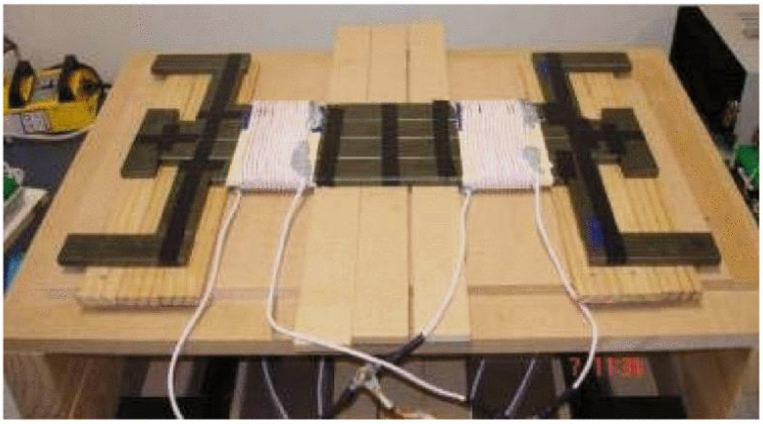

Figure 1. Prototype flux tube concept with coils in parallel.

Figure 2. Photograph of the 3 kw transformer.

In 2013, the University of Auckland proposed a design scheme called the “DDQ” coil. This coil consists of two coils: a transmitting coil and a receiving coil. The transmitting coil adopts a DD-type coil, as shown in Figure 3, while the receiving coil utilizes a coil known as the DDQ coil, as shown in Figure 4. The distinguishing feature of this design is that the magnetic field directions are opposite, while the current directions at the center conductor are the same, resulting in enhanced magnetic field and improved displacement tolerance for electric vehicles. However, this design also faced the issue of magnetic field zero points. Subsequently, researchers introduced a modified design called the "DDD coil", which addressed the problem of magnetic field zero points. The DDD coil design effectively resolved the issue while reducing coil losses [7]. A. Zaheer proposed a design scheme for a bipolar BP coil, as shown in Figure 5. Compared to the DDQ coil, this design can reduce coil losses while achieving similar functionality [11]. In 2014, South Korea proposed a design scheme for a three-coil structure, as shown in Figure 6. This design consists of three coils, with one large coil nested inside a smaller coil. This design enhances the coil's resistance to interference and improves its stability [12].

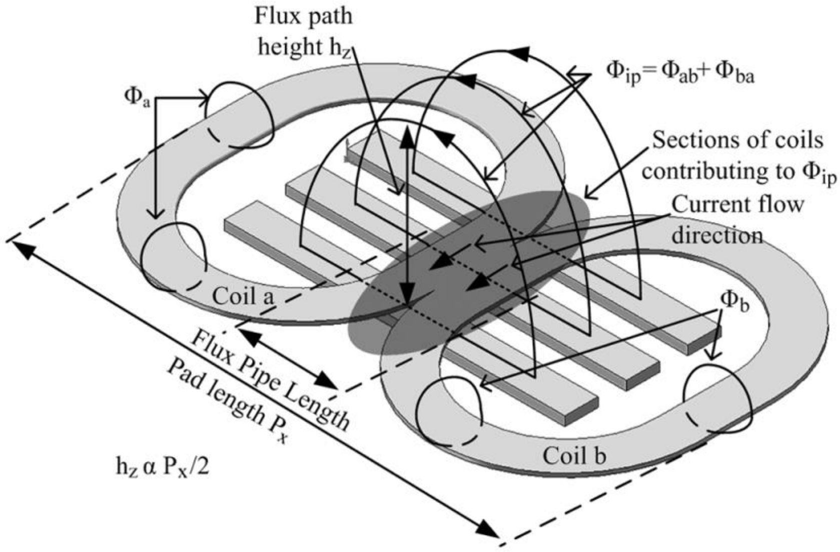

Figure 3. Simplified model of a DD pad.

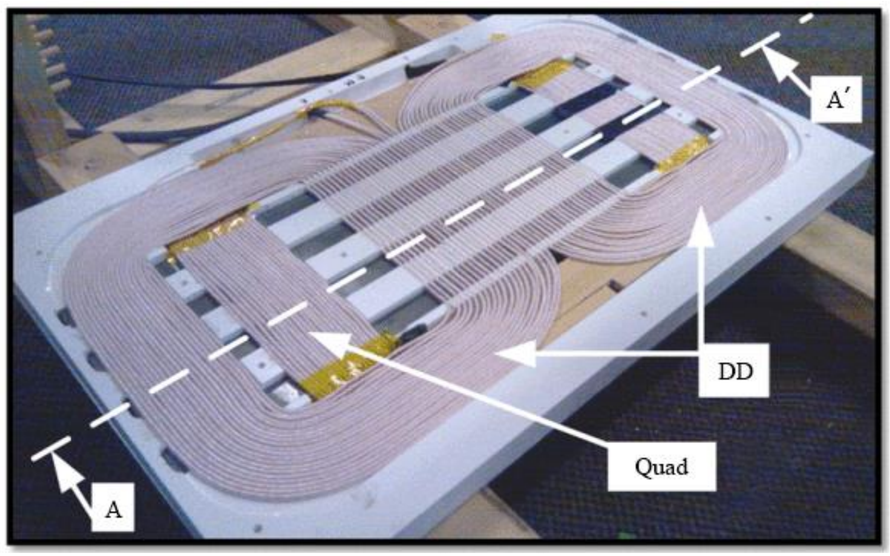

Figure 4. DD-Q pads with built receiver.

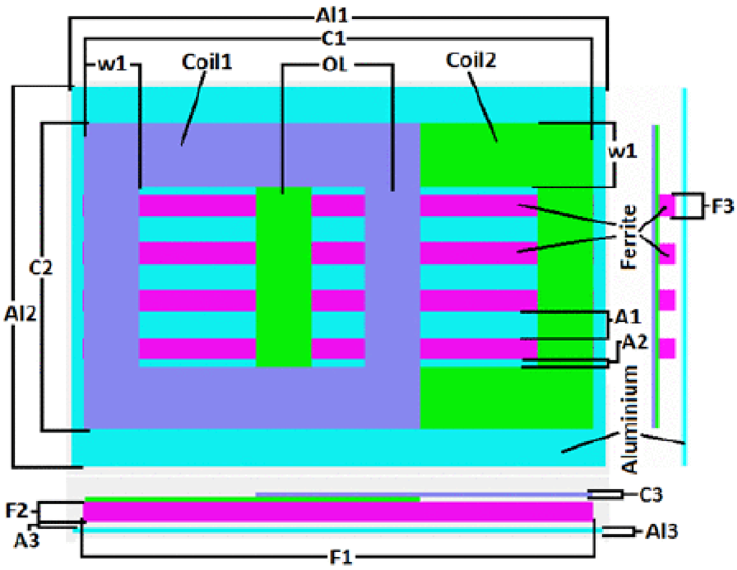

Figure 5. BPP construction.

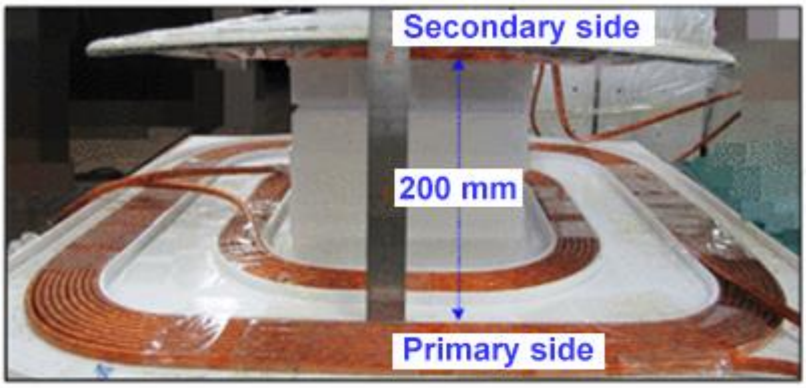

Figure 6. Three-coil structure.

In 2017, the University of Auckland proposed a design scheme called the TPP coil, as shown in Figure 7. Unlike traditional coil designs, the TPP coil utilizes a unique magnetic circuit structure that enhances the coil's resistance to displacement [13]. In 2019, the Tianjin University of Technology proposed a design called the "Taiji coil", based on the DD coil, as shown in Figure 8. The Taiji coil demonstrates similar transmission efficiency to circular coils and DD coils when in the centered position. However, in the misaligned state, it achieves a higher coupling coefficient, resulting in improved transmission efficiency. This demonstrates that the Taiji coil possesses better misalignment tolerance [14].

Nowadays, many types of couplers have been developed, such as square coils, circular pad, four square coils, DD couplers and DDQ couplers [4,5]. A comparison between circular and elliptical coils is made by studying the shape of the magnetic field and the path of the magnetic flux with a flux pipe concept [5,6]. The experimental results show that the coupling coefficient of the circular pad and DD coupling coils is higher and the cost is lower with respect to the coil type. Two analytical models of square and circular planar spiral coils were developed to compare their differences [10]. The results show that the square coil is a better choice for pad design when the outer diameter of the circular coil is equal to the outer side length of the square coil [15]. The characteristics of the coil structure are shown in Table 1.

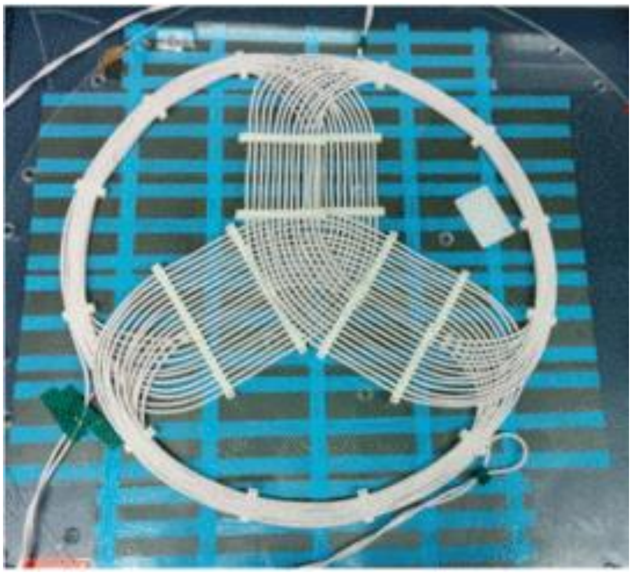

Figure 7. Prototype of TPP.

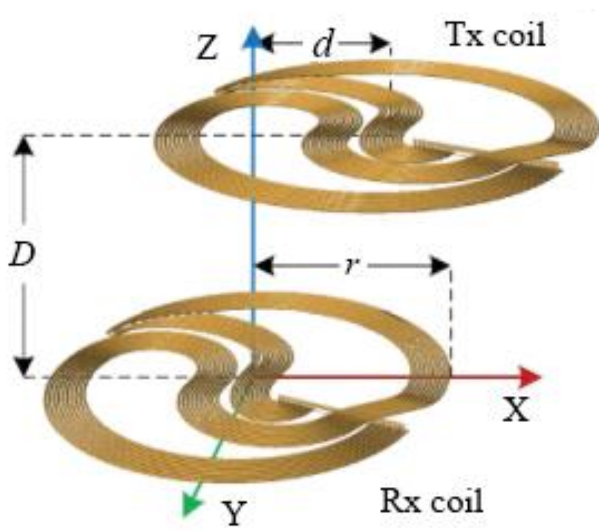

Figure 8. Taichi coil.

Table 1. The characteristics of coil structure.

Coil Type	Offset Resistance	Magnetic Leakage	Losses (nH)	Coefficient (%)
Flux pipe	better	larger	larger	42 (offset)
H	better	larger	larger	90
DD	better	smaller	average	95.66
DDQ	better	smaller	smaller	95
BP	average	smaller	smaller	92.85

The above papers present specific coil designs and analyses based on the experience of the authors. There is no basic design guide. All kinds of more complex coils are composed of the two basic coil structures, circular and square. In this paper the problems of which is the better choice between circular and square structure and which one is more favorable to the system will be studied using basic circular and square coils. We encountered the above coil design problem when designing a wirelessly powered electromagnetic coupling mechanism for an electric bus. Our experimental subject was a Yutong ZK6875BEVG pure electric bus with a permanent magnet synchronous motor model YTM280-CV4-H.

For the two most common types of circular and square coils, the structure is axisymmetric. For each of the above two types of coils as the transmitting coil, the case of magnetic field coupling using two types of single-turn coils as the receiving coil is considered, as shown in Figure 9. First, the calculation models of the magnetic induction intensity of two kinds of coils were established, numerical calculations were carried out via MATLAB R2020b, and then the electromagnetic coupling characteristics of the two coils as receiving coils under three different conditions were qualitatively analyzed. Secondly, the simulation analysis of three kinds of couplers, a coupler with two circular loops (circular coupler), a coupler with one circular and one square loop (hybrid coupler), and a coupler with two square loops (square coupler), were carried out in Ansoft Maxwell 16.0 electromagnetic simulation software. Finally, the analysis was verified experimentally, and the characteristics of the two types of coils and the occasions for adjustment were obtained. The significance of this paper is that it establishes a reference for basic structural options that can be integrated into the selection and design of coil structures.

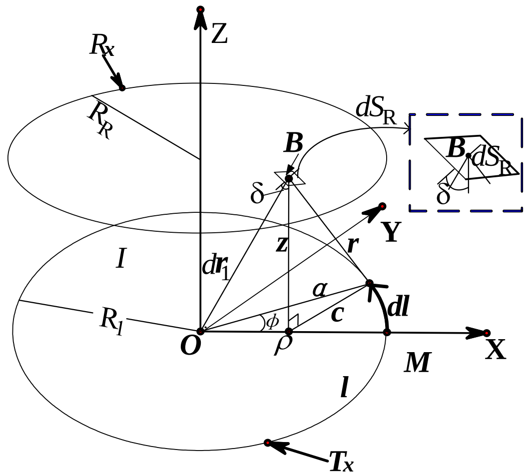

(**a**) A circular coupler.

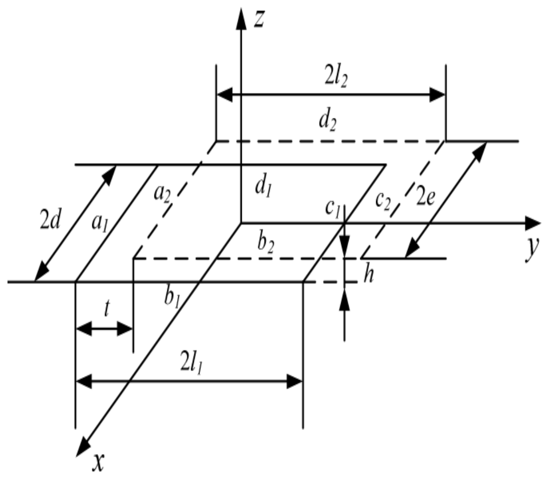

(**b**) A rectangular coupler.

Figure 9. Single-loop coupler.

2. Modeling and Analysis

For a given coil, according to Biot–Savart's law, the magnetic flux density of a line segment can be written as

$$\vec{B} = \mathrm{N_R N_T} \frac{\mu_0 I(t)}{4\pi} \oint_l \frac{dl \times \vec{r}}{r} \tag{1}$$

where N_R and N_T are the turns of the receiving and transmitting coils, respectively, *I(t)* is the current carried by the transmitting coil, *dl* is the micro-element on the wire, and *r* is the distance from the micro-element to one point in space.

2.1. Derivation of Circular Coil Magnetic Flux Density

The magnetic flux density $\vec{B}$ of the circular transmitting coil at any point in space is independent of the φ coordinate due to the symmetry [16], as shown in Figure 9a.

$$\vec{B} = B_\rho \hat{\rho} + B_z \hat{z} \tag{2}$$

$$\mathrm{B}_z|_{\rho=0} = \frac{\mu_0 I(t) a^2}{2(a^2+z^2)^{3/2}} \tag{3}$$

$$\mathrm{B}_z|_{\rho\neq 0} = \frac{\mu_0 I(t)}{2\pi\rho}\left(\frac{m}{4a\rho}\right)^{1/2}\left(\rho K(m) + \frac{am-(2-m)\rho}{2(1-m)}E(m)\right) \tag{4}$$

$$\mathrm{B}_\rho = \frac{\mu_0 I(t) z}{2\pi\rho}\left(\frac{m}{4a\rho}\right)^{1/2}\left(\frac{2-m}{2(1-m)}E(m) - K(m)\right) \tag{5}$$

$$\begin{cases} K(m) = \int_0^{\pi/2} \frac{d\theta}{\sqrt{1-m\ \sin^2\theta}} \\ E(m) = \int_0^{\pi/2} \sqrt{1-m\ \sin^2\theta}\, d\theta \\ m = \frac{4a\rho}{z^2+(a+\rho)^2} \end{cases} \tag{6}$$

where $\mathrm{B_r}, \mathrm{B_z}$ are the coordinate component of *B*. *a*, *z*, and ρ are the length of the line in Figure 9a. In Figure 9a, $\mathrm{R_x}$ is the receiving coil, $\mathrm{R_R}$ is the radius of $\mathrm{R_x}$, and the rest of the symbols are lengths or angles.

2.2. Derivation of Square Coil Magnetic Flux Density

The magnetic flux density at any point resulting from a line of finite length can be expressed as in [17], as shown in Figure 9b.

$$B_l = \frac{\mu_0 I}{4\pi\rho}\left(\frac{d+x}{\sqrt{\rho^2+(d+x)^2}} + \frac{d-x}{\sqrt{\rho^2+(d-x)^2}}\right) \tag{7}$$

where *d* is the side length of square coil and ρ is the distance from one point to the line segment. For a square coil, the magnetic flux density $\vec{B}$ can be expressed as

$$\vec{B} = \vec{B}_\mathrm{a} + \vec{B}_\mathrm{b} + \vec{B}_\mathrm{c} + \vec{B}_\mathrm{d} \tag{8}$$

where the subscripts a, b, c, and d represent the segments of the corresponding square coil.

2.3. Qualitative Analysis of Electromagnetic Properties

For the transmitting coils with a given surrounding area of 0.28 m^2, according to (2) and (8), the normalized curve of the magnetic flux density can be obtained when the circular and square coils are used as the transmitting coils, respectively, as shown in Figure 10. In Figure 10, the horizontal axis is the horizontal distance from any point of constant height to the central axis of the transmitter coil. The height of the measuring point is 0.25 m from the coils. It can be seen from Figure 10 that the B value is higher inside the coils and gradually decreases outside the coils.

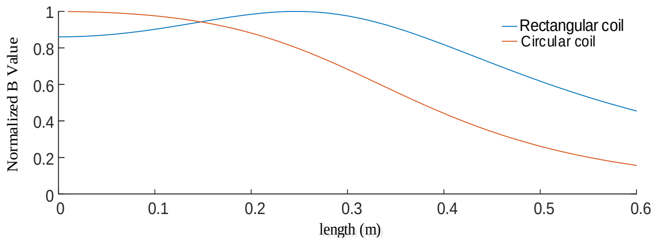

Figure 10. Normalized magnetic flux density curve.

For the circular and square loops serving as receiving coils, there are three scenarios: (1) the enclosed area of the two receiving coils is the same; (2) the circumference of the two receiving coils is the same; (3) the outer diameter of the two receiving coils is the same, as depicted in Figure 11a, b, and c, respectively.

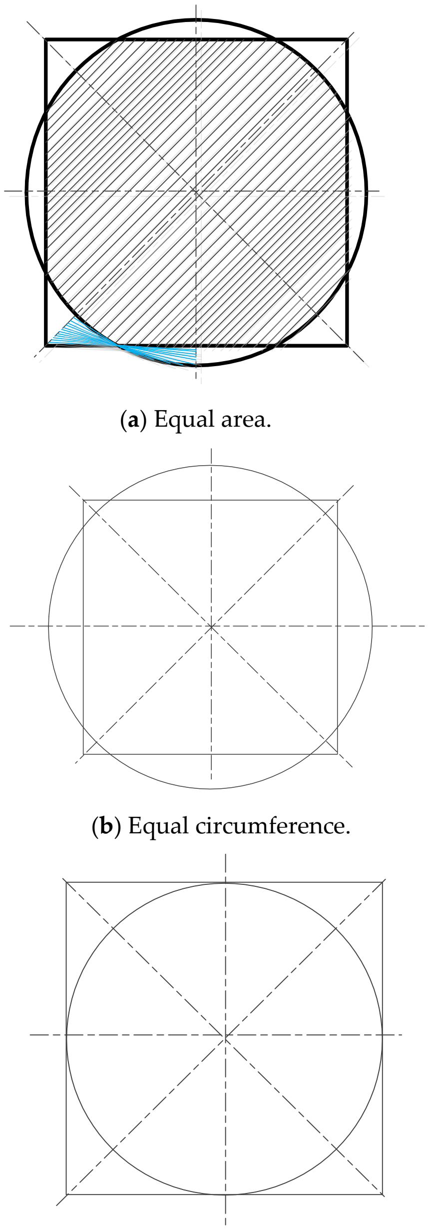

(**a**) Equal area.

(**b**) Equal circumference.

(**c**) Equal outer diameter.

Figure 11. Comparison of three cases.

In the case of an equal surrounding area, the girth ratio is $\sqrt{\pi}/2$, as shown in Figure 11a. The lightly shaded area is the overlap of the two receiving coils. It is obvious that the magnetic flux of the two receiving coils is the same in this part. Due to symmetry, the dark shaded area of the two receiving coils is the same. According to the conclusion of the electromagnetic induction characteristics of the transmitting coil in Figure 10, the magnetic flux of the circular receiving coil is greater than or equal to that of the square receiving coil in the dark shaded area. Therefore, for circular and square receiving coils with the same surrounding area, the magnetic flux of the circular receiving coil should be greater than or equal to that of the square receiving coil.

For the case of the same perimeter as shown in Figure 11b, the area ratio is $4/\pi$. According to the above analysis result, the magnetic flux of the circular receiving coil is greater than that of the square receiving coil because the surrounded area of the circular receiving coil is larger than that of the square receiving coil.

In the case of the same outer diameter, as shown in Figure 11c, all of the area and circumference ratio is $\pi/4$. The magnetic flux of the circular receiving coil is smaller than that of the square receiving coil because the surrounded area of the circular receiving coil is smaller than that of the square receiving coil.

3. Numerical Simulations

The results of the above analysis are compared by simulating the mutual inductance of the coils using electromagnetic simulation software.

3.1. Normalized Coupling Coefficient Comparison

The results of the qualitative analysis show that the equal surrounded area result is in the middle of the other two results, so it is a key point of comparison for circular and square coils. Clear results can be obtained by analyzing circular and square coils of equal enveloping area. Figure 12 shows the simulation of normalized coupling coefficients for the same enveloping area of circular, hybrid, and square couplers of the three coupler types. The horizontal axis is the horizontal distance between the center of the transmitting coil and the center of the receiving coil. The size of the square loop is 0.3 m $\times$ 0.3 m in length and width, and the radius of the circular loop is 0.17 m. The height of the two coupling coils in the simulation is fixed at 0.3 m. The simulation results show that the coupling coefficient is highest for the circular coupler and lowest for the square coupler, i.e., the coupling coefficient of the circular coupler is higher than that of the square coupler. These results are consistent with the qualitative analysis above.

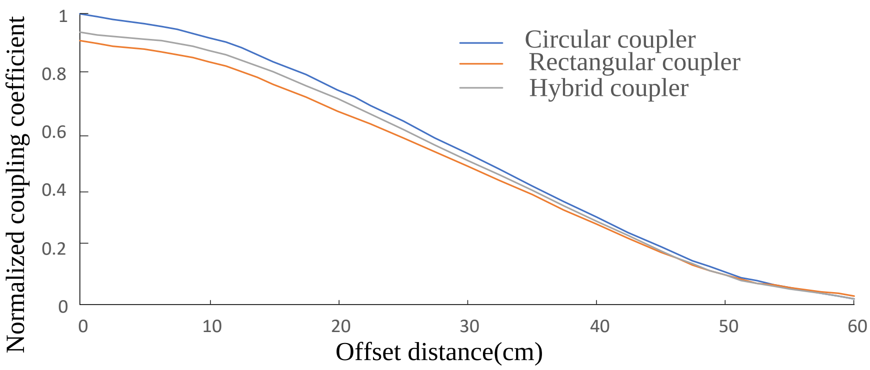

Figure 12. Normalized coupling coefficient curve.

3.2. Coupling Mutual Inductance Comparison

Table 2 shows the mutual inductances in the surrounding area of 0.09 m^2, 0.16 m^2, and 0.25 m^2 of circular coupler, hybrid coupler, and square coupler, respectively. It can clearly be seen that the mutual inductance and coupling coefficient of the coupler with the circular loop are larger than that with the square loop.

Table 2. Comparison of different area couplers s.

Coil Type	Pacing (m)	Area (m^2)	Mutual Inductance (nH)	Coupling Coefficient (%)
circular	0.3	0.09	30	2.52
hybrid			29	2.4
rectangular			28	2.23
circular		0.16	67.5	4.13
hybrid			66.9	3.94
rectangular			65.5	3.75
circular		0.25	120	5.62
hybrid			119.19	5.4
rectangular			117.5	5.15

In Table 3, a square loop with a length of 0.3 m is used as a reference, and the circular and square loops are, respectively, used as the transmitting coil and the receiving coil to simulate the nine kinds of structure of the coupler with the same surrounded area, the same circumference, and the same outer diameter, respectively.

Table 3. Detailed simulation data comparison of couplers.

<table>
<tr><th>Coil Type</th><th>Pacing (m)</th><th>Area (m²)</th><th>Perimeter (m)</th><th>Outer Diameter (m)</th><th>Mutual Inductance (nH)</th><th>Coupling Coefficient (%)</th></tr>
<tr><td>circular</td><td rowspan="9">0.3</td><td rowspan="3">0.09</td><td>1.06</td><td>0.34</td><td>30</td><td>2.52</td></tr>
<tr><td>hybrid</td><td></td><td></td><td>29</td><td>2.4</td></tr>
<tr><td>rectangular</td><td>1.2</td><td>0.3</td><td>28</td><td>2.23</td></tr>
<tr><td>circular</td><td>0.11</td><td rowspan="3">1.2</td><td>0.38</td><td>42.22</td><td>3.12</td></tr>
<tr><td>hybrid</td><td></td><td></td><td>34.95</td><td>2.69</td></tr>
<tr><td>rectangular</td><td>0.09</td><td>0.3</td><td>28</td><td>2.23</td></tr>
<tr><td>circular</td><td>0.07</td><td>0.94</td><td rowspan="3">0.3</td><td>19.99</td><td>1.97</td></tr>
<tr><td>hybrid</td><td></td><td></td><td>23.7</td><td>2.1</td></tr>
<tr><td>rectangular</td><td>0.09</td><td>1.2</td><td>28</td><td>2.23</td></tr>
</table>

It can be seen from Table 2 that the mutual inductance of the circular coupler is greater than that of a square coupler. The concept of the self-inductance coefficient is employed to compare the difference between the coils of two couplers. The self-inductance of the circular coil, the mutual inductance, and the coupling coefficient of the circular coupler are set as L_1, M_1, and $K_{1,}$ respectively. The self-inductance of the square coil, the mutual inductance, and the coupling coefficient of the square coupler are set as L_2, M_2, and K_2, respectively. The mutual inductance and the coupling coefficient of the hybrid coupler are set to M_3 and K_3, respectively.

The proportional relationship of the self-inductance of the coupled structure is obtained.

$$\frac{\sqrt{L_i L_j}}{\sqrt{L_k L_m}} = \frac{M_s K_t}{M_t K_s} \tag{9}$$

where $i, j, k, m \in (1,2)$, $s = \begin{cases} i, & i = j \\ 3, & i \neq j \end{cases}$, $t = \begin{cases} k, & k = m \\ 3, & k \neq m \end{cases}$.

For a set of coupling structures of equal surrounded area in Table 2, the self-inductance coefficient of a circular coupler and square coupler can be obtained from (9):

$$\frac{L_1}{L_2} = \frac{M_1K_2}{M_2K_1} \approx 0.95 \tag{10}$$

For a set of coupling structures of the same perimeter in Table 2, the self-inductance coefficient of a circular coupler and square coupler can be obtained from (9):

$$\frac{L_1}{L_2} = \frac{M_1K_2}{M_2K_1} \approx 1.08 \tag{11}$$

According to the data in Table 2 and the contrast between (10) and (11), it can be obtained that self-inductance is not only affected by the line length but also closely related to the structure. For the same length, the self-inductance of the circular coil inductance is larger than that of the square one.

4. Experimental Validation

In order to verify the theoretical and simulation results, we set up an experimental platform for three kinds of coupler.

Based on the above discussion, it can be seen that the results obtained under the condition that the square coil and the circular coil surround the same area are the watersheds of the three cases. If the results of equal area are obtained under the same conditions, the other two results are clear.

In this experiment, the outer diameter, wire diameter, and number of turns of the circular coil are 15.6 cm, 2.5 mm, and five turns, respectively. The self-inductance of the two circular coils is 7.49 uH and 7.42 uH, respectively. The outer diameter, wire diameter, and number of turns of the square coil are 13.8 cm, 2.5 mm, and five turns, respectively. The self-inductance of the two regulation coils is 7.49 uH and 7.42 uH, respectively.

The experimental platform is shown in Figure 13. The mutual inductance calculation method can be performed by measuring two coils in series and subtracting two self-inductances [13]. The experimental data and results are shown in Table 4. Table 3 lists the mutual inductance and coupling coefficients of the three types of couplers at three different pitches for the transmitter and receiver coils. Figure 14 shows the verification system for this experiment. Figure 15 shows the wireless power supply system and coil that we developed for the electric vehicle.

Table 4. Experimental data on equal surrounded areas.

Coil Type	Pacing (mm)	Mutual Inductance (uH)	Coupling Coefficient (%)
circular	67.82	0.857	11.5
hybrid		0.844	11.21
rectangular		0.735	9.66
circular	79.17	0.609	8.17
hybrid		0.607	8.06
rectangular		0.593	7.8
circular	105.17	0.332	4.46
hybrid		0.329	4.37
rectangular		0.326	4.29

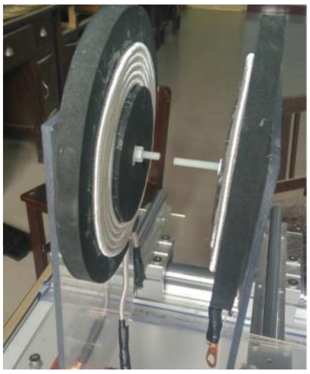

(**a**) Equal area.

(**b**) Equal circumference.

(**c**) Equal outer diameter.

Figure 13. Comparison of three cases of experimental coils.

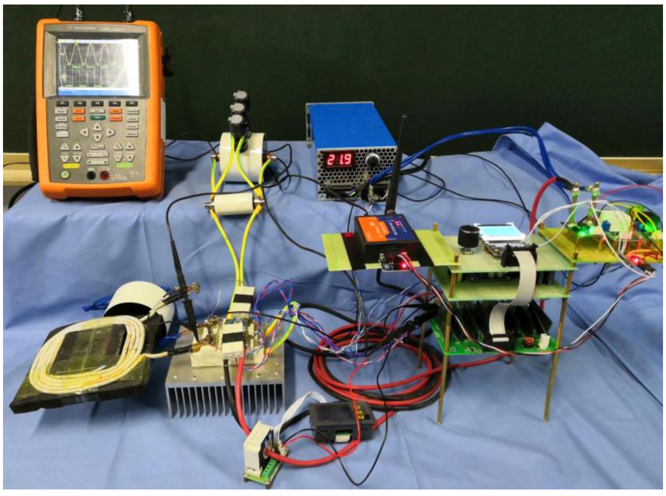

Figure 14. The experimental system.

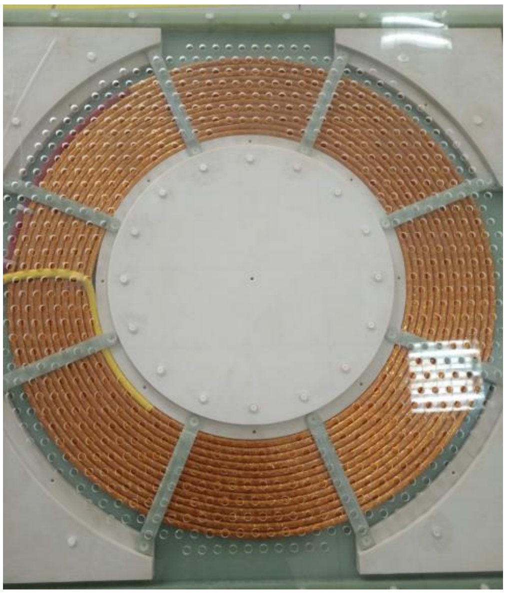

(**a**) Designed wireless power transfer coils for EV.

(**b**) Design of a wireless power supply transmitter for EV.

Figure 15. The wireless power supply system for EV.

5. Discussion of the Electromagnetic Characteristics of Two Basic Coil Shapes

According to the characteristic curve of the magnetic induction intensity of the transmitting coils, the electromagnetic coupling characteristics of the circular and square loops as the receiving coil under three different conditions were qualitatively analyzed by comparing the magnetic fluxes of the two coils for equal surrounded area, equal circumference, and equal outer diameter, respectively. The qualitative analysis result for equal surrounded area is in the middle of the other two results, so it is a key point of comparison for circular and square loops. Therefore, the simulation analysis is mainly based on the same surrounded area conditions of circular and square loops. Secondly, three kinds of coupler are simulated with the coil of equal surrounded area. The simulation results show that the mutual inductance coupling coefficient of the coupler with the circular loop is larger than that with the square coil. Finally, the mutual inductances of the three kinds of coupler for different surrounded area are compared, and the mutual inductances of the three kinds of coupler for the same surrounded area, the same circumference, and the same outer diameter are simulated, respectively. The final results show that the qualitative analysis and simulation analysis are highly consistent.

6. Conclusions

Through the above analysis, the circular coil flux is greater than the square coil flux in the case of equal surrounded area or equal perimeter. Namely, in these two cases, the circular receiving coil mutual inductance is greater than that of the square receiving coil. The cost and loss of the circular and square coil are equal when the circumference is equal. The mutual inductance of the circular coil is clearly better than that of the square coil, so the efficiency is higher. When the enclosed area is equal, the cost and loss of the circular coil is lower than that of the square coil, and the mutual inductance is slightly larger than that of the square coil, so the efficiency is also higher than that of the square coil. Therefore, it is best to choose a circular coil with no space constraints. Under the condition of limited space, the square coil can achieve greater mutual inductance, but the cost and loss of the coil will be higher than that of the circular coil. The above conclusions provide the basis for the development of more reasonable and efficient composite couplers by using the basic structure.

Author Contributions: Conceptualization, J.Z. and T.C.; methodology, Y.Z. and J.Z.; software, L.Z. and J.Z.; validation, Y.Z.; writing—original draft preparation, J.Z.; writing—review and editing, L.Z. All authors have read and agreed to the published version of the manuscript.

Funding: This work was supported by the National power grid headquarter science and technology project (funding number 5201011600TW).

Data Availability Statement: Some or all data and models generated or used during the study are available in a repository or online.

Conflicts of Interest: The authors declare no conflict of interest. Tianjin Chen is an employee of Xuji Power Co., Ltd. The paper reflects the views of the scientists and not the company.

References

1. Zhao, Z.; Liu, F.; Chen, K. New progress of wireless charging technology for electric vehicles. *Trans. China Electrotech. Soc.* **2016**, *31*, 30–40. (In Chinese)
2. Assawaworrarit, S.; Yu, X.; Fan, S. Robust wireless power transfer using a nonlinear parity-time-symmetric circuit. *Nature* **2017**, *546*, 387. [CrossRef] [PubMed]
3. Kurs, A.; Karalis, A.; Moffatt, R.; Joannopoulos, J.D.; Fisher, P.; Soljacic, M. Wireless power transfer via strongly coupled magnetic resonances. *Science* **2007**, *317*, 83–86. [CrossRef] [PubMed]
4. Zhao, J.F.; Huang, X.L.; Wang, W. Efficiency analysis of magnetic resonance wireless power transfer with three-dimensional transmitters. *J. Appl. Phys.* **2015**, *117*, 83. [CrossRef]
5. Wake, K.; Laakso, I.; Hirata, A.; Chakarothai, J.; Onishi, T.; Watanabe, S.; De Santis, V.; Feliziani, M. Derivation of Coupling Factors for Different Wireless Power Transfer Systems: Inter- and Intralaboratory Comparison. *IEEE Trans. Electromagn. Compat.* **2017**, *59*, 677–685. [CrossRef]
6. Wang, Y.; Yao, Y.; Liu, X.; Xu, D. S/CLC Compensation Topology Analysis and Circular Coil Design for Wireless Power Transfer. *IEEE Trans. Transp. Electrif.* **2017**, *3*, 496–507. [CrossRef]
7. Budhia, M.; Boys, J.T.; Covic, G.A.; Huang, C.-Y. Development of a Single-Sided Flux Magnetic Coupler for Electric Vehicle IPT Charging Systems. *IEEE Trans. Ind. Electron.* **2013**, *60*, 318–328. [CrossRef]
8. Budhia, M.; Covic, G.A.; Boys, J.T. Design and optimization of circular magnetic structures for lumped inductive power transfer systems. *IEEE Trans. Power Electron.* **2011**, *26*, 3096–3108. [CrossRef]
9. Budhia, M.; Covic, G.; Boys, J. A new IPT magnetic coupler for electric vehicle charging systems. In Proceedings of the IECON 2010—36th Annual Conference on IEEE Industrial Electronics Society, Glendale, AZ, USA, 7–10 November 2010; pp. 2487–2492.
10. Takanashi, H.; Sato, Y.; Kaneko, Y.; Abe, S.; Yasuda, T. A large air gap 3 kW wireless power transfer system for electric vehicles. In Proceedings of the Energy Conversion Congress and Exposition, Raleigh, NC, USA, 15–20 September 2012; pp. 269–274.
11. Zaheer, A.; Kacprzak, D.; Covic, G.A. A bipolar receiver pad in a lumped IPT system for electric vehicle charging applications. In Proceedings of the 2012 IEEE Energy Conversion Congress and Exposition (ECCE), Raleigh, NC, USA, 15–20 September 2012; pp. 283–290.
12. Moon, S.; Kim, B.-C.; Cho, S.-Y.; Ahn, C.-H.; Moon, G.-W. Analysis and Design of a Wireless Power Transfer System with an Intermediate Coil for High Efficiency. *IEEE Trans. Ind. Electron.* **2014**, *61*, 5861–5870. [CrossRef]
13. Kim, S.; Covic, G.A.; Boys, J.T. Tripolar Pad for Inductive Power Transfer Systems for EV Charging. *IEEE Trans. Power Electron.* **2017**, *32*, 5045–5057. [CrossRef]
14. Li, Y.; Zhao, J.; Yang, Q.; Liu, L.; Ma, J.; Zhang, X. A Novel Coil with High Misalignment Tolerance for Wireless Power Transfer. *IEEE Trans. Magn.* **2019**, *55*, 2800904. [CrossRef]

15. Luo, Z.; Wei, X. Analysis of Square and Circular Planar Spiral Coils in Wireless Power Transfer System for Electric Vehicles. *IEEE Trans. Ind. Electron.* **2018**, *65*, 331–341. [CrossRef]
16. Zhao, J.; Huang, X.; Wang, W. Wireless power transfer with two-dimensional resonators. *IEEE Trans. Magn.* **2014**, *50*, 1–4. [CrossRef]
17. Zhao, J. Research on Three-Dimensional Wireless Power Transmission System. Ph.D. Thesis, Southeast University, Nanjing, China, 2015. (In Chinese)